Noise-sustained propagation of unstable pulses due to exponential interaction between pulse fronts in bistable systems with flows

Yo Horikawa* and Hiroyuki Kitajima

Faculty of Engineering, Kagawa University, Takamatsu 761-0396, Japan
(Received 4 January 2010; published 7 April 2010)

We study effects of noise on pulse propagation in two bistable systems with flows: a chain of unidirectionally coupled neurons and a reaction-diffusion-convection equation with cubic nonlinearity. Pulse propagation in the systems is described by a common kinematical equation, which has exponential interaction between adjacent pulse fronts. The propagation length of pulses is then dealt with as a first passage time problem on it. We show that additive spatiotemporal noise increases the propagation length of unstable pulses and sustains pulse propagation. The mean propagation length of a single pulse increases infinitely in the presence of noise of infinitesimal strength. The propagation length of a pulse is distributed in a power-law form of exponent $-3/2$ as noise strength increases. A resonancelike behavior is also shown by bounding pulse width, and the mean propagation length is maximal at intermediate noise strength. Further, the proportion of survival pulses at some fixed length takes a maximum value at optimal noise strength.

I. INTRODUCTION

Spatiotemporal stochastic resonance in spatially extended systems, e.g., excitable media and coupled oscillators, has attracted much attention in various fields [1]. One of its forms is noise-sustained propagation of patterns and signals [2]. That is, spatiotemporal noise supports the propagation of signals in media, and the signal-to-noise ratio (SNR) is maximized at some optimal noise strength. It was first reported in spiral waves in two-dimensional excitable media, in which it was shown that noise sustains spiral growth and controls its scale in a two-dimensional coupled array of threshold elements [3]. Concerning coupled bistable systems, noise enhanced signal propagation has been shown in coupled bistable electronic elements [4], one-way coupled bistable systems [5], one- and two-dimensional arrays of two-way coupled bistable oscillators [6], nonlinear lines of coupled noisy threshold elements [7], and a chain of forward-coupled bistable overdamped oscillators [8]. In continuous bistable media, it has been shown that multiplicative noise sustains the propagation of unstable pulses in a reaction-diffusion-convection equation [9].

In this study, we consider noise-sustained pulse propagation in two kinds of one-dimensional bistable systems with flows. One is a chain of unidirectionally coupled sigmoidal neurons and the other is a scalar reaction-diffusion-convection equation with cubic nonlinearity. These spatially discrete and continuous systems have qualitatively the same kinematics of pulse propagation and decay. We can then treat the two systems with a common kinematical model.

Concerning a chain of neurons, dynamics of a ring of unidirectionally coupled neurons (a ring neural network) has been widely studied [10]. It has been shown that a ring neural network has unstable oscillations for some parameter values, which are traveling waves rotating in the network. Re-

cently, we derived a kinematical equation describing the traveling waves and showed that the duration of oscillations increases exponentially with the number of neurons [11]. Further, it was shown that the duration of oscillations increases in the presence of spatiotemporal noise of intermediate strength [12]. An open chain of unidirectionally coupled neurons can work as a signal transmission line. Pulses can propagate in a chain with the same mechanism as a ring neural network, while they are unstable and disappear eventually. It is expected that the propagation length of pulses increases in the presence of noise in the same manner as a ring neural network.

Concerning a reaction-diffusion-convection equation, it has been shown that a bistable reaction-diffusion equation with symmetric cubic nonlinearity shows metastable dynamics of kink and pulse patterns [13]. The motion of kinks and pulses is extremely slow, and the speeds of them decrease exponentially with the length of domains and the width of pulses. The duration of these transient patterns increases exponentially with system sizes consequently. Recently, we showed that the duration of kinks in one-dimensional bounded domains increases in the presence of spatiotemporal noise of intermediate strength [14]. In the presence of convection, pulses propagate with decays until disappearing, so that signals can be transmitted over some length. Noise is then expected to increase the propagation length of pulses. Although it has been shown that multiplicative noise sustains pulse propagation in a reaction-diffusion-convection equation [9], it is expected that additive noise also sustains pulse propagation with another mechanism.

As mentioned above, the propagation and decay of pulses in the two systems are expressed with common kinematics. There is attractive interaction between adjacent pulse fronts, which is expressed with an exponential of an interval between pulse fronts [11,13]. Further, spatiotemporal noise causes random fluctuations in the locations and widths of pulses [12,14]. Changes in pulse width during propagation are then described kinematically by the first-order ordinary differential equation with a fluctuation term. The propagation

---

*Corresponding author. FAX: +81-87-864-2262;
horikawa@eng.kagawa-u.ac.jp
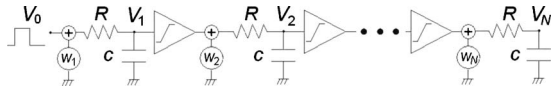
FIG. 1. Analog circuit of a chain of neurons.

length of pulses is obtained by first passage time (FPT) for the stochastic kinematical equation. Numerical calculations of the integral formulas of the FPT show that the mean propagation length of pulses diverges to infinity in the presence of noise. It is also shown with computer simulation with the original models and kinematical equations that the probability density function of the propagation length of pulses has a power-law form of exponent $-3/2$. This power-law form is the same as that of the Wiener process and is due to the fact that the strength of the interaction between pulse fronts decreases exponentially with pulse width. By imposing an upper bound of pulse width, it is shown that there is optimal noise strength for sustaining pulse propagation. Further, the number of surviving pulses in an asymmetric pulse train is also maximized by noise of intermediate strength depending on propagation length.

In the following, a chain of neurons and a reaction-diffusion-convection model with kinematics of propagating pulses are explained in Sec. II. Increases in the propagation length of a single pulse and a pulse train due to noise are shown in Sec. III. Conclusion is then given in Sec. IV. In the Appendix, two equivalent stochastic processes with multiplicative noise are derived from the kinematical equation of pulse propagation.

II. BISTABLE SYSTEMS WITH FLOWS AND PULSE KINEMATICS

A. Chain of unidirectionally coupled sigmoidal neurons

First, we consider the following chain of unidirectionally coupled neurons of sigmoidal input-output relations with additive noise:

$$du_n(t)/dt = -u_n(t) + \tanh[gu_{n-1}(t)] + \sigma_c w_n(t)$$
$$(g > 1, \quad 1 \le n \le N)$$

$$u_0(t) = u_p \quad (0 < t < \tau_s), \quad = -u_p$$
$$(\text{otherwise}) \quad [u_p = \tanh(gu_p) > 0]$$

$$u_n(0) = -u_p \quad (0 \le n \le N)$$

$$E\{w_n(t)\} = 0, \quad E\{w_n(t)w_{n'}(t')\} = \delta_{nn'} \cdot \delta(t - t') \qquad (1)$$

where u_n is the state of the nth neuron, N is the number of neurons, $\tanh(gu)$ is the sigmoidal output function of neurons, and g is an output gain. Figure 1 shows an analog circuit of Eq. (1), in which voltages V_n at capacitances correspond to the states u_n of neurons. Neurons are unidirectionally coupled in a chain and the output of each neuron is transmitted to the next neuron. Gaussian white noise $w_n(t)$ with strength σ_c is also added to each neuron independently. The zeroth state $u_0(t)$ is regarded as input to a chain. When
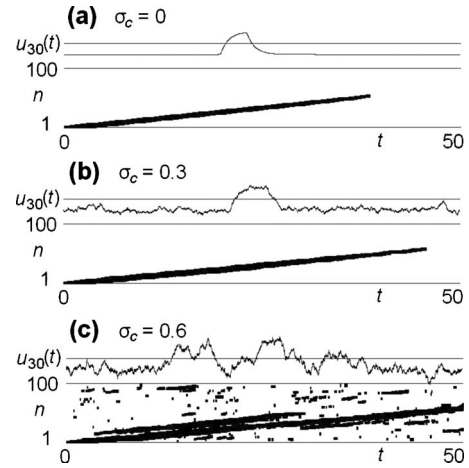
FIG. 2. Spatiotemporal patterns of the states of neurons in a chain Eq. (1) of $N=100$ and $g=10.0$ with $\sigma_c=0.0$ (a), $\sigma_c=0.3$ (b), $\sigma_c=0.6$ (c) for an input pulse of $\tau_s=4.0$. Upper panels: time courses of $u_{30}(t)$. Lower panels: the states of neurons (positive: black, negative: white).

the output gain is larger than unity ($g>1$), a chain is bistable in the absence of noise. That is, when input is $u_0(t)=\pm u_p$, where $u_p=\tanh(gu_p)(>0)$, the states of all neurons take the same values as $u_n(t)=\pm u_p(0 \le n \le N)$. In Eq. (1), the negative steady states $-u_p$ is the resting states of neurons, and an input pulse of height u_p and width τ_s is added to the first neuron. A pulse is transmitted to the following neurons so that it propagates in a chain. However, it decays during propagation and eventually disappears when $N \gg 1$ so that the states of all neurons return to the resting states $-u_p$. Noise gives random fluctuations in the speeds of pulse fronts and the width of a pulse during propagation, and hence it varies the propagation length of a pulse.

Figure 2 shows examples of propagating pulses in a chain of neurons obtained with computer simulation. Numerical calculation of Eq. (1) was done using the Euler method with a time step 0.01. The values of parameters are: $N=100$, $g=10.0$, $\tau_s=4.0$, and the strength of noise is changed as $\sigma_c=0.0$ (a), 0.3 (b), and 0.6 (c). Time courses of the state $u_{30}(t)$ of the 30th neuron are plotted in upper panels. Black and white regions in lower panels correspond to the states of neurons of positive and negative signs, respectively, in which pulses propagate from bottom to top. A pulse disappears at $n \approx 55$ in the absence of noise (a). The trajectory and propagation length of a pulse vary in the presence of noise ($\sigma_c=0.3$) (b). Variations in the states of neurons increase so that pulses can be generated spontaneously and the bistability of a chain tends to be lost as noise strength increases further ($\sigma_c=0.6$) (c).

The propagation time and speed of a pulse front depend on an exponential of an interval between it and the preceding pulse front. Let $t_0(n)$ be time at which a forward front of a pulse passes the nth neuron, which is defined by time at which the state of the xth neuron crosses zero, i.e., $u_n[t_0(n)]=0$. Also let $t_1(n)$ be time at which a backward front passes the nth neuron $\{u_n[t_1(n)]=0\}$. The propagation time $\Delta t_0(n)$ of a forward front and that $\Delta t_1(n)$ of a backward front at the nth neuron, which are time required for the propaga-

tion of the fronts over one neuron, are obtained in the same way as a ring neural network [11,12,15],

$$\Delta t_0(n) = \log 2 + 2^{-1/2}\sigma_c w_n$$

$$\Delta t_1(n) = \log 2 + \log[1 - \exp\{-[t_1(n) - t_0(n)]\}] + 2^{-1/2}\sigma_c w_n'$$

$$E\{w_n\} = E\{w_n'\} = 0, \quad E\{w_n w_{n'}\} = E\{w_n' w_{n'}'\}$$

$$= \delta_{nn'}, \quad E\{w_n w_{n'}'\} = 0 \quad (2)$$

where w_n and w_n' are Gaussian white noise. Let a spatial location x be a continuum limit of the number n of neurons. Changes in temporal pulse width $\tau(x) = t_1(x) - t_0(x)$ at the xth neuron are then obtained as

$$d\tau(x)/dx \approx \Delta t_1(x) - \Delta t_0(x) = \log 2 + \log\{1 - \exp[-\tau(x)]\}$$

$$+ 2^{-1/2}\sigma_c w_n - [\log 2 + 2^{-1/2}\sigma_c w_n']$$

$$\approx -\exp[-\tau(x)] + \sigma_c w(x) \quad (0 \le x \le N)$$

$$\tau(0) = \tau_s, \quad E\{w(x)\} = 0, \quad E\{w(x)w(x')\} = \delta(x - x') \quad (3)$$

where $w(x)$ is Gaussian white noise along the trajectories of pulse fronts. The N-dimensional differential equation [Eq. (1)] is reduced to the scalar differential equation describing the motion of a pulse.

B. Reaction-diffusion-convection equation

Next, we consider the following reaction-diffusion-convection equation with symmetric cubic nonlinearity in a one-dimensional domain [9]:

$$\partial u/\partial t = \partial^2 u/\partial x^2 - c_0 \, \partial u/\partial x + u(1 - u^2) + \sigma_r w \quad (0 < x < L)$$

$$u(0,t) = u_0(t), \quad u(x,0) = -1, \quad \partial u(L,t)/\partial x = 0$$

$$u_0(t) = 1 \quad (0 < t < \tau_s), \quad = -1 \quad (\text{otherwise})$$

$$E\{w(x,t)\} = 0, \quad E\{w(x,t)w(x',t')\} = \delta(x - x')\delta(t - t') \quad (4)$$

where $w(x,t)$ is Gaussian spatiotemporal white noise. A reaction-diffusion equation without convection ($c_0 = 0$) in Eq. (4) is known as the time-dependent Ginzburg-Landau equation [13] or the Schlögl model [16] in the field of phase transitions and has been widely studied. The system is bistable ($u = \pm 1$) in the absence of noise ($\sigma_r = 0$), and transient kinks and pulses can exist, the motion of which is exponentially slow with domain length and pulse width. Let a pulse (a kink-antikink pair) exist in an infinite domain ($-\infty < x < \infty$), and let l_L be the location of a left front (a kink) and l_R be the location of a right front (an antikink). That is, $u > 0$ for $l_L < x < l_R$, and $u < 0$ otherwise. Changes in the spatial width $l = l_R - l_L$ of a pulse is described as [13,14]

$$dl(t)/dt = dl_R(t)/dt - dl_L(t)/dt$$

$$= -48\sqrt{2}\exp(-\sqrt{2}l(t)) + (9/8)^{1/4}\sigma_r w(t)$$

$$- \{48\sqrt{2}\exp(-\sqrt{2}l(t)) + (9/8)^{1/4}\sigma_r w'(t)\}$$

$$= -24\sqrt{2}\exp(-\sqrt{2}l(t)) + (9/2)^{1/4}\sigma_r w(t) \quad (5)$$
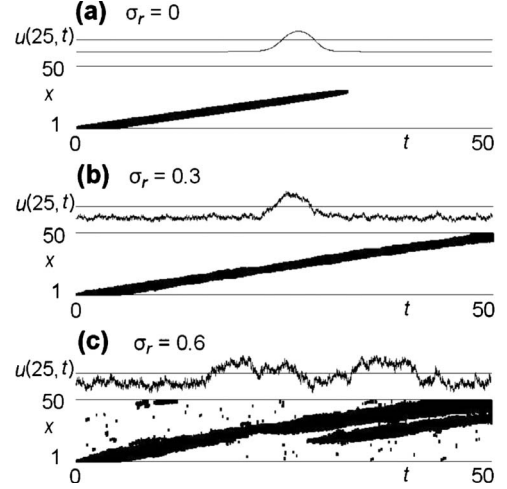
FIG. 3. Spatiotemporal patterns of the states u in a reaction-diffusion-convection equation [Eq. (4)] of $L = 50$ and $c_0 = 1.0$ with $\sigma_c = 0.0$ (a), $\sigma_c = 0.3$ (b), $\sigma_c = 0.6$ (c) for an input pulse of $\tau_s = 5.0$. Upper panels: time courses of $u(25,t)$. Lower panels: the signs of the states (positive: black, negative: white).

where $w(t)$ and $w'(t)$ are Gaussian white noise, and noise strength $(9/2)^{1/4}\sigma_r$ is derived according to [16].

In the presence of convection, a constant speed c_0 is added to the motion of a pulse. When an input pulse $u_0(t)$ of width τ_s is added at $x = 0$, it propagates over some length owing to convection while it is unstable and disappears eventually. The propagation of a pulse is dealt with simply by taking a moving coordinate $x' = x - c_0 t$ so that Eq. (4) reduces to the reaction-diffusion equation without convection. Changes in the temporal width $\tau(x)$ of a pulse during propagation is described by adding c_0 to dl_L/dt and dl_R/dt in Eq. (5) and taking the inverses of them with $l = c_0\tau$ as

$$d\tau(x)/dx = 1/(dl_L(t)/dt) - 1/(dl_R(t)/dt)$$

$$= 1/[c_0 + 48\sqrt{2}\exp(-\sqrt{2}c_0\tau(x)) + (9/8)^{1/4}\sigma_r w'(x)]$$

$$- 1/[c_0 - 48\sqrt{2}\exp(-\sqrt{2}c_0\tau(x)) + (9/8)^{1/4}\sigma_r w(x)]$$

$$\approx -24\sqrt{2}c_0^{-2}\exp(-\sqrt{2}c_0\tau(x))$$

$$+ (9/2)^{1/4}c_0^{-2}\sigma_r w(x) \quad (0 < x < L)$$

$$\tau(0) = \tau_s, \quad E\{w(x)\} = 0, \quad E\{w(x)w(x')\} = \delta(x - x') \quad (6)$$

where $w(x)$ and $w'(t)$ are Gaussian white noise along the trajectories of pulse fronts.

Figure 3 shows examples of propagating pulses in Eq. (4) obtained with computer simulation. Numerical calculation of Eq. (4) was done using the Euler method with a space step 0.2 and a time step 0.01. The values of parameters are: $L = 50.0$, $c_0 = 1.0$, $\tau_s = 5.0$, and the strength of noise is changed as $\sigma_r = 0.0$ (a), 0.3 (b), and 0.6 (c). Time courses of the state $u(25,t)$ at $x = L/2$ are plotted in upper panels, and black and white regions in lower panels correspond to the state u of positive and negative signs respectively. Spatiotemporal patterns are similar to those in a chain of neurons in Fig. 2. A pulse disappears at $x \approx 30$ in the absence of noise (a), the trajectory of a pulse varies and it reaches L in the presence of

small noise (σ_r=0.3) (b), and variations in the state u are so large that it is hard to discriminate a pulse in the presence of large noise (σ_r=0.6) (c).

III. INCREASES IN THE PROPAGATION LENGTH OF PULSES DUE TO NOISE

A. Single pulses

As shown in Sec. II, changes in temporal pulse width $\tau(x)$ at a spatial location x during propagation in both of a chain of neurons (CN) and a reaction-diffusion-convection (RDC) equation are described by

$$d\tau(x)/dx = -\beta \exp[-\alpha\tau(x)] + \sigma w(x) \quad (x > 0)$$

$$\tau(0) = \tau_s, \quad E\{w(x)\} = 0, \quad E\{w(x)w(x')\} = \delta(x - x')$$

$$\beta = 1, \quad \alpha = 1, \quad \sigma = \sigma_c \quad \text{(CN)}$$

$$\beta = 24\sqrt{2}c_0^{-2}, \quad \alpha = \sqrt{2}c_0, \quad \sigma = (9/2)^{1/4}c_0^{-2}\sigma_r \quad \text{(RDC)}.$$
$$(7)$$

In the absence of noise (σ=0), the solution of Eq. (7) is given by

$$\tau(x) = \frac{\log[\exp(\alpha\tau_s) - \beta\alpha x]}{\alpha} \tag{8}$$

which tends to negative infinity in a finite time. The propagation length x_p of a pulse is obtained by solving $\tau(x_p)$=0 as

$$x_p(\tau_s; \sigma = 0) = \frac{\exp(\alpha\tau_s) - 1}{\alpha\beta} \quad [\tau(x_p) = 0] \tag{9}$$

which increases exponentially with initial pulse width τ_s. This exponentially long propagation with initial pulse width is due to the exponentially small deterministic term in Eq.
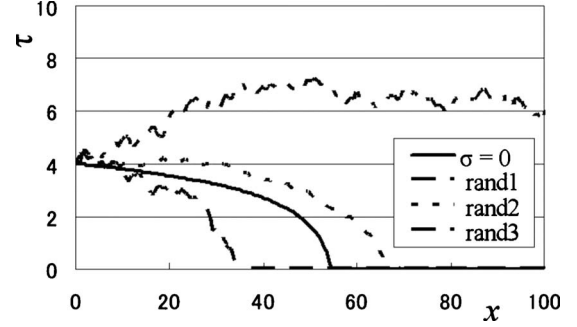
FIG. 4. Sample paths of pulse width $\tau(x)$ in Eq. (7) with $\alpha=\beta=1$ (CN) and τ_s=4.0.

(7). In the presence of noise (σ>0), the propagation length of a pulse is regarded as FPT for Eq. (7) with $\tau(x_p)$=0, in which the meanings of space and time are interchanged from conventional use in stochastic processes. Figure 4 shows sample paths of temporal pulse width $\tau(x)$ in Eq. (7) with $\alpha=\beta=1$ (CN) and τ_s=4.0. Equation (7) was numerically calculated using the Euler method with a time step 0.01. A solid line denotes a path in the absence of noise, in which pulse width becomes zero at $x \approx 54$ as in Fig. 2(a). In the presence of noise, the propagation length of a pulse decreases (a dashed line) or increases (a dotted line), and a pulse sometimes sustains for long length (a dash-dotted line). Since the deterministic term in Eq. (7) decreases exponentially as pulse width increases, large pulse width behaves like the Wiener process (a one-dimensional random walk or Brownian motion), in which the mean FPT (the recurrence time) is infinite [17]. Hence, once pulse width becomes large owing to noise, it hardly tends to decrease to zero.

The mean $m(x_p(\tau_s))$ of the propagation length of a pulse of initial width $\tau(0)=\tau_s$ is expressed by the following integral formula [18]:

$$m(x_p(\tau_s)) = 2\int_0^{\tau_s} \pi(\eta)d\eta \int_\eta^\infty 1/(b(\xi)\pi(\xi))d\xi = \frac{2}{\sigma^2}\int_0^{\tau_s} d\eta \int_\eta^\infty d\xi \exp\left\{\frac{2\beta[\exp(-\alpha\xi) - \exp(-\alpha\eta)]}{\alpha\sigma^2}\right\}$$

$$\pi(\tau) = \exp\left[-\int^\tau \frac{2a(\eta)}{b(\eta)}d\eta\right] = \exp\left[\frac{-2\beta\exp(-\alpha\tau)}{\alpha\sigma^2}\right]$$

$$a(\tau) = -\beta\exp(-\alpha\tau), \quad b(\tau) = \sigma^2 \tag{10}$$

where $a(\tau)$ and $b(\tau)$ correspond to the deterministic term and the variance of noise respectively in Eq. (7). The double integral in the first equation diverges to infinity for finite noise strength (σ>0) since the double exponential function $1/\pi(\xi)$ does not converge to zero in the limit of $\xi\to\infty$ [$\pi(\infty)\to1$]. That is, the mean propagation length of a pulse increases infinitely in the presence of noise. This

divergence of the mean propagation length resembles that of the mean FPT in the Wiener process [$a(\tau)$=0 and $b(\tau)=\sigma^2$], in which $\pi(\tau)$=1 so that the definite integral from η to ∞ of $1/\pi(\xi)$ tends to infinity. It occurs when a deterministic term $a(\tau)$ approaches zero faster than $O(1/\tau)$ as $\tau\to\infty$ so that $\pi(\xi\to\infty)$>0, even though $a(\tau)$<0 and propagation length x_p is finite in the absence of noise.
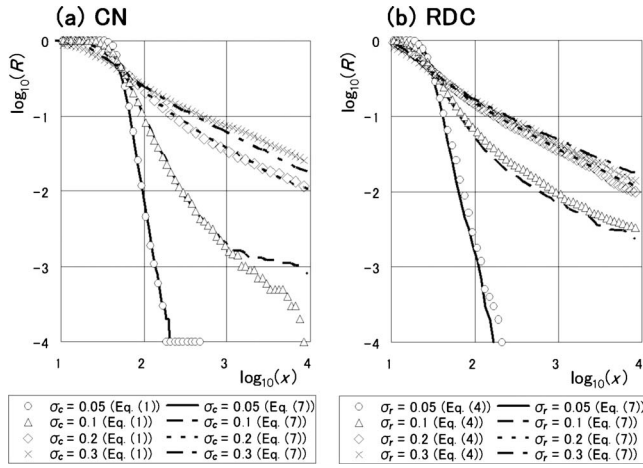
FIG. 5. Survival function $R(x)$ of the propagation length of a pulse for (a) CN and (b) RDC. Results of computer simulation with Eqs. (1) and (4) (symbols) and with Eq. (7) (lines).

We then consider the survival function $R(x)$, which is the probability that a pulse propagates over length x and is defined by

$$R(x) = \int_x^\infty f(x_p)dx_p = 1 - F(x) \qquad (11)$$

where $f(x_p)$ and $F(x_p)$ are the probability density function and the cumulative distribution function of propagation length x_p respectively. Figure 5 shows a log-log plot of the survival function $R(x)$ of the propagation length of a pulse for (a) CN and (b) RDC. Plotted are estimates with 10 000 trials of computer simulation with the original equations [Eqs. (1) and (4)] (symbols) and with the kinematical equation [Eq. (7)] (lines). Initial pulse width τ_s is 4.0 in CN and 5.0 in RDC, the number N of neurons (the length of a chain) in Eq. (1) and domain length L in Eq. (4) are 10 000, and noise strength is changed as $\sigma_c = \sigma_r = 0.05$, 0.1, 0.2, and 0.3. As noise strength increases, a tail of the survival function becomes in a form of the inverse half power of x as $R(x) \propto x^{-1/2}$. The probability density function $f(x_p)$ then takes a form of $x_p^{-3/2}$, which is the same as that of FPT in the Wiener process (the positive stable distribution of order 1/2) [17]. The simulation results of Eq. (7) agree with those of Eqs. (1) and (4).

It should be noted that the propagation length $x_p \approx 24.51$ for $\tau_s = 5.0$ (RDC) in Eq. (9) is slightly smaller than the length ($x_p = 30.4$) obtained by computer simulation with Eq. (4) in RDC in the absence of noise. The difference ($= 5.9$) is added to values of propagation length obtained with computer simulation of Eq. (7) in RDC here and below. This deviation is due to the limitations of the kinematical approach, in which some approximations are applied, e.g., the approximation of a sigmoidal output function of neurons by a sign function [11,12] and that of a pulse form by a superposition of a kink-antikink pair [13]. As a result, there are differences by several percent between simulation results of the original equations and estimates derived from the kine-

FIG. 6. Integral Eq. (12) with $\alpha = \beta = 1$ vs noise strength σ for $\tau_s = 4.0$, 6.0, 8.0, 10.0 (a). Optimal noise strength σ_o at the maxima of Eq. (12) vs initial pulse width τ_s (a solid line) and the maximal points (τ_m, σ_m) [Eq. (13)] (a dashed line) in a contour map of $\log_{10}(2\pi(\tau)/\sigma^2)$ in the $(\tau, \log_{10}\sigma)$ plane with $\alpha = \beta = 1$ (b).

matical models in the duration of oscillations in a ring neural network [11] and that of kinks in a bistable reaction-diffusion equation [14].

While the mean propagation length increases infinitely for infinitesimal noise strength, a resonancelike phenomenon exists intrinsically. The double integral for $m[x_p(\tau_s)]$ in Eq. (10) is dominated by the integral with respect to η in the limit of $\xi \to \infty$ and is formally proportional to it.

$$m(x_p(\tau_s)) \propto \int_0^{\tau_0} \frac{2}{\sigma^2}\exp\left[\frac{-2\beta\exp(-\alpha\tau)}{\alpha\sigma^2}\right]d\eta$$

$$= \int_0^{\tau_0} 2\pi(\tau)/\sigma^2 d\eta. \qquad (12)$$

Figure 6(a) shows numerically calculated integral Eq. (12) with $\alpha = \beta = 1$ as a function of noise strength σ for $\tau_s = 4.0$, 6.0, 8.0, 10.0. The graphs have the maxima, at which noise strength is optimal for increasing the mean propagation length. Further, the noise strength σ_o at the maximum decreases as initial pulse width τ_s increases. In Fig. 6(b), the optimal noise strength σ_o at the maximum of Eq. (12) against initial pulse width τ_s is plotted in the $(\tau, \log_{10}\sigma)$ plane (a solid line). The optimal noise strength σ_o decreases exponentially with initial pulse width τ_s. This exponential relation is

derived by considering a form of the integrand $2\pi(\tau)/\sigma^2$ in Eq. (12). A contour map of $\log_{10}(2\pi(\tau)/\sigma^2)$ in the (τ, $\log_{10}\sigma$) plane with $\alpha=\beta=1$ is also plotted in Fig. 6(b), in which a black region corresponds to the smallest values. There are the maximal points (τ_m, σ_m) in $2\pi(\tau)/\sigma^2$ with respect to σ for fixed τ, at which contour lines are vertical. Further, they coincide with the inflection points with respect to τ for fixed σ, at which $2\pi(\tau)/\sigma^2$ increases rapidly with τ. That is, these points satisfy the exponential relation

$$\sigma^2 = 2k/\alpha \cdot \exp(-\alpha\tau) \quad \{\partial[2\pi(\tau)/\sigma^2]/\partial\sigma = 0,$$
$$\partial^2[2\pi(\tau)/\sigma^2]/\partial\tau^2 = 0\}. \quad (13)$$

For small noise strength ($\sigma \ll 1$), the integrand $2\pi(\tau)/\sigma^2$ increases exponentially with τ from a small value $2/\sigma^2 \cdot \exp[-2k/(\alpha\sigma^2)]$ ($\ll 1$) at $\tau=0$ and is saturated to $2/\sigma^2$ ($\gg 1$) as τ increases. Hence, the integral Eq. (12) for fixed τ_s is maximized near σ satisfying Eq. (13) with $\tau=\tau_s$. The maximal points (τ_m, σ_m) [Eq. (13)] is also plotted in Fig. 6(b) with a dashed line, which is close to the line of the maximal points (τ_s, σ_o) of Eq. (12) (a solid line). The slopes of them agree with each other and it is equal to $-\alpha/2$ in Eq. (13). Thus the optimal variance σ_o^2 of noise is proportional to the value of the deterministic term $\exp(-\alpha\tau_s)$ with $\tau=\tau_s$ in Eq. (7) and also about to the inverse of the propagation length $x_p(\tau_s;\sigma=0)$ [Eq. (9)] in the absence of noise.

The resonancelike behavior in the mean propagation length is manifested by imposing a finite boundary condition as a ring neural network. That is, we consider the propagation length of a pulse at which temporal pulse width becomes zero or a fixed value $\tau_B(>\tau_s)$. It corresponds to FPT for Eq. (7) from τ_s to 0 or τ_B [the life time of the process $\tau(x)$ before it is absorbed at the boundaries $\tau=0$ or τ_B]. The mean propagation length $m(x_p(\tau_s);\tau_B)$ under this condition is given by

$$m[x_p(\tau_s);\tau_B] = 2\left\{\int_0^{\tau_s}\pi(\eta)d\eta\int_\eta^{\tau_B}1/[b(\xi)\pi(\xi)]d\xi\right.$$
$$\left. + p(\tau_B|\tau_0)\int_0^{\tau_B}\pi(\eta)d\eta\int_\eta^{\tau_B}1/[b(\xi)\pi(\xi)]d\xi\right\}$$

$$p(\tau_B|\tau_s) = \int_0^{\tau_s}\pi(\eta)d\eta / \int_0^{\tau_B}\pi(\eta)d\eta \quad (14)$$

where $p(\tau_B|\tau_s)$ is the probability that τ ever reaches τ_B, and $\pi(\tau)$, $a(\tau)$ and $b(\tau)$ are given in Eq. (10) [18]. The probability $p(\tau_B|\tau_s)$ decreases to zero as τ_B increases, and $m(x_p(\tau_s);\tau_B)$ in Eq. (14) agrees with $m(x_p(\tau_s))$ in Eq. (10) in the limit of $\tau_B\to\infty$. Figure 7 shows the mean propagation length $m(x_p(\tau_s);\tau_B)$ as a function of noise strength for (a) CN and (b) RDC. Initial pulse width τ_s is 4.0 and a bounded value τ_B is 10.0 in CN, and they are 5.0 and 10.0 respectively in RDC. Plotted are estimates with 10000 trials of computer simulation with Eqs. (1) and (4) (solid circles) and numerical integrals of Eq. (14) (solid lines). [The difference 5.9 is added to the numerical integral of Eq. (14) in RDC as noted above.] The mean propagation length
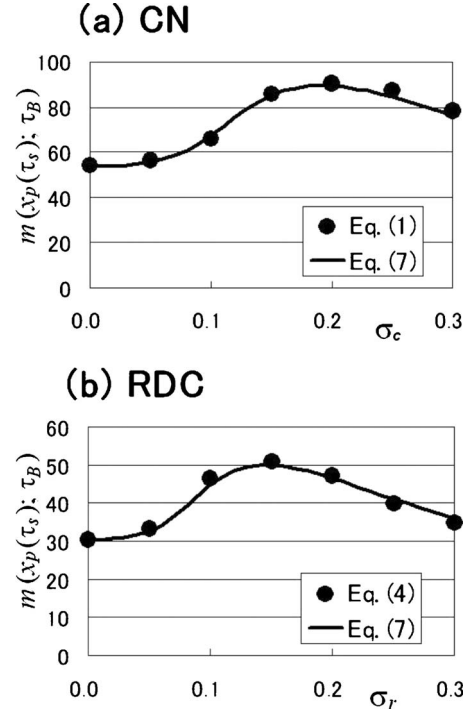
FIG. 7. Mean propagation length $m(x_p(\tau_s);\tau_B)$ vs noise strength for CN with $\tau_s=4.0$ and $\tau_B=10.0$ (a) and RDC with $\tau_s=5.0$ and $\tau_B=10.0$ (b). Estimates with 10 000 trials of computer simulation with Eqs. (1) and (4) (solid circles) and numerical integrals of Eq. (14) (solid lines).

increases at intermediate noise strength. The numerical integrals of Eq. (14) agree with the simulation results of the original equations. The optimal noise strength at the maximum in CN is about 0.2, which is close to that ($\sigma_o \approx 3.0$) at the maximum of Eq. (12) for $\tau_s=4.0$ in Fig. 6(a) (a solid line). It can be shown that the optimal noise strength increases to σ_o as the upper bound τ_B of pulse width increases.

Such increases in the mean FPT due to noise never occur in well-known related stochastic processes, e.g., the Wiener process with drift and the Ornstein-Uhlenbeck process, in which the mean FPT decreases monotonically with noise strength [19]. The increase in the propagation length of a pulse is due to exponential nonlinearity in the deterministic term in the kinematical equation [Eq. (7)]. Further, Eq. (7) is transformed to simple stochastic processes with multiplicative noise, which is derived in the APPENDIX. Hence, multiplicative noise can work for increasing FPT intrinsically.

B. Pulse trains

We then consider the transmission of a pulse train in the systems. Instead of a single pulse, let a pulse train be added to the first neuron (CN) and at $x=0$ (RDC) as

$$u_0(t) = -u_+ \quad (t_{2k-1} < t < t_{2k}) = u_+ \quad (t_{2k} < t < t_{2k+1})$$
$$(k \geq 0, \quad t_0 = 0, \quad t_{-1} = -\infty) \quad (15)$$

where $u_+=u_p$ in CN and $u_+=1$ in RDC. A propagating pulse train alternating between u_+ and $-u_+$ is then generated. Let

(a)

(b)
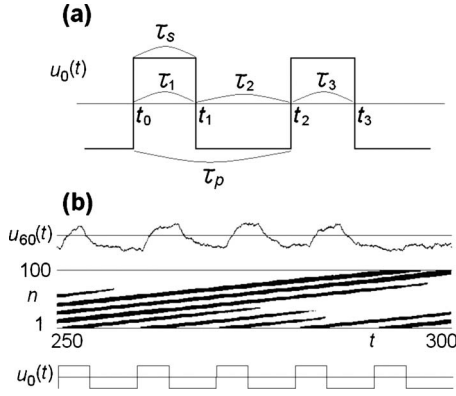
FIG. 8. (a) Asymmetric periodic input pulse train $u_0(t)$ in Eqs. (15)–(17). (b) Spatiotemporal patterns of the states of neurons in CN with $N=100$, $g=10.0$ and $\sigma_c=0.2$ for an input pulse train $u_0(t)$ in Eqs. (15)–(17) with $\tau_p=10.0$ and $\tau_s=4.0$. Top panel: time course of $u_{60}(t)$. Middle panel: states of neurons (positive: black, negative: white). Bottom panel: time course of $u_0(t)$.

the temporal widths of positive and negative pulses be $\tau_j = t_j - t_{j-1}$ of odd and even j, respectively [Fig. 8(a)]. According to [15], the pulse kinematics [Eq. (7)] is extended to a pulse width sequence $\tau_j(x)$ as

$$d\tau_j(x)/dx = -\beta\{\exp[-\alpha\tau_j(x)] - \exp[-\alpha\tau_{j-1}(x)]\}$$
$$+ \sigma/\sqrt{2} \cdot [w_j(x) - w_{j-1}(x)] \quad (x > 0)$$

$$\tau_j(0) = t_j - t_{j-1} \quad (j \geq 1), \quad \tau_0(0) = \infty$$

$$E\{w_j(x)\} = 0, \quad E\{w_j(x)w_{j'}(x')\} = \delta_{j,j'}\delta(x-x') \quad (j,j' \geq 0) \tag{16}$$

where $w_j(x)$ is Gaussian white noise along the trajectories of the jth pulse fronts.

Let us consider a periodic pulse train with a period τ_p and the width of positive pulses τ_s [Fig. 8(a)]

$$\tau_{2k-1}(0) = \tau_s, \quad \tau_{2k}(0) = \tau_p - \tau_s \quad (k \geq 1). \tag{17}$$

It can be shown that positive pulses disappear at finite length when the width of positive pulses is smaller than that of negative pulses ($\tau_s < \tau_p/2$) and the system beyond it remains the negative steady state, while positive pulses merge with each other (negative pulses disappear) when $\tau_s > \tau_p/2$ and the system beyond it changes to the positive steady state. In the absence of noise, the propagation length of a pulse train in a stationary state ($j \to \infty$) is obtained in the same way as a ring neural network [11] as

$$x_p(\tau_s, \tau_p; \sigma=0) = 1/(\alpha\beta) \cdot \exp(\alpha\tau_p/2)\{\text{arctanh}\{\exp[\alpha(\tau_s - \tau_p/2)]\} - \text{arctanh}[\exp(-\alpha\tau_p/2)]\} \tag{18}$$

which agrees with Eq. (9) in the limit of $\tau_p \to \infty$. When a pulse train is symmetric ($\tau_s = \tau_p/2$), the propagation lengths of pulses increase one by one to infinity, and noise just destabilizes pulse propagation. When a pulse train is asymmetric ($\tau_s \neq \tau_p/2$), however, noise can support the propagation of pulses.

Computer simulation of Eq. (1) (CN) and Eq. (4) (RDC) with input Eqs. (15) and (17) was done for an asymmetric pulse train with $\tau_p=10.0$ and $\tau_s=4.0$ (CN) and $\tau_p=12.0$ and $\tau_s=5.0$ (RDC), in which $\tau_s < \tau_p/2$ and positive pulses disappear during propagation.

Figure 8(b) shows an example of a propagating pulse train in CN, in which $u_0(t)$, $x_n(t)$ ($1 \leq n \leq 100$) and $u_{60}(t)$ are plotted from bottom to top.

When the jth pulse disappears, the two adjacent $j \pm 1$st pulses merge and the number of pulses is reduced by two. Computer simulation of kinematical Eq. (16) with Eq. (17) was also done under the condition that the widths of the successive two pulses ($\tau_j(x)$ and $\tau_{j+1}(x)$) are added to the j-first pulse width $\tau_{j-1}(x)$ and pulses after $j+2$nd are renumbered when the width of the jth pulse decreases to zero ($\tau_j(x) \leq 0$). The number of positive pulses in input was 10 000 (10 000 periods) in each run. Figure 9 shows the proportion $R_n(x)$ of the number of remaining pulses to the number of input pulses, i.e., the proportion of survival pulses, verses propagation length x in (a) CN and (b) RDC with $\sigma_c=\sigma_r=0$, 0.05, 0.15, and 0.3 (upper panels). Plotted are results of computer simulation with the original equations [Eqs. (1) and (4)] (symbols) and those with the kinematical equation [Eq. (16)] (lines). Since $\tau_s < \tau_p/2$, positive pulses disappear at $x \approx 54$ (CN) and $x \approx 30$ (RDC) in the absence of noise, which are about the same as the propagation lengths $x_p(\tau_s; \sigma=0)$ of single pulses, and the proportions $R_n(x)$ of survival pulses suddenly change from unity to zero (open circles and solid lines). As noise strength increases, the slope of the graph of $R_n(x)$ becomes gradual, and pulses disappear faster at small length but remain longer at large length. The simulation results of Eq. (16) agree with those of Eqs. (1) and (4). The proportion of survival pulses at $x=60$ in (a) CN and $x=35$ in (b) RDC, which are just beyond the propagation length in the absence of noise, are also plotted as a function of noise strength (lower panels). They increase at intermediate noise strength ($\sigma_c=\sigma_r \approx 0.1 \sim 0.2$) in both systems although there are some differences between the results of computer simulation of the original equations and Eq. (16). As can be seen from the graphs in upper panels, the proportion $R_n(x)$ of survival pulses decreases monotonically with noise strength at smaller length than $x_p(\tau_s; \sigma=0)$, but it once increases as noise strength increases at longer length. The optimal noise strength depends on propagation length and increases with it.

It can be shown that the proportion $R_n(x)$ of survival pulses in an asymmetric pulse train is about the same as the survival function $R(x)$ of a single pulse (Fig. 5) for not so large length ($x < 100$). As x increases, pulses of large width that were made by merging with the adjacent pulses become dominant in a pulse train so that the proportion of survival pulses becomes larger than $R(x)$. It can also be shown that the proportion of survival pulses at fixed length in a pulse train with random pulse width takes a maximum value at intermediate noise strength, while its increase is small. Although this diffusionlike phenomenon is easily expected from the viewpoint of the FPT problem for stochastic processes, it seems to have never been pointed out in studies on noise-sustained signal propagation in bistable systems
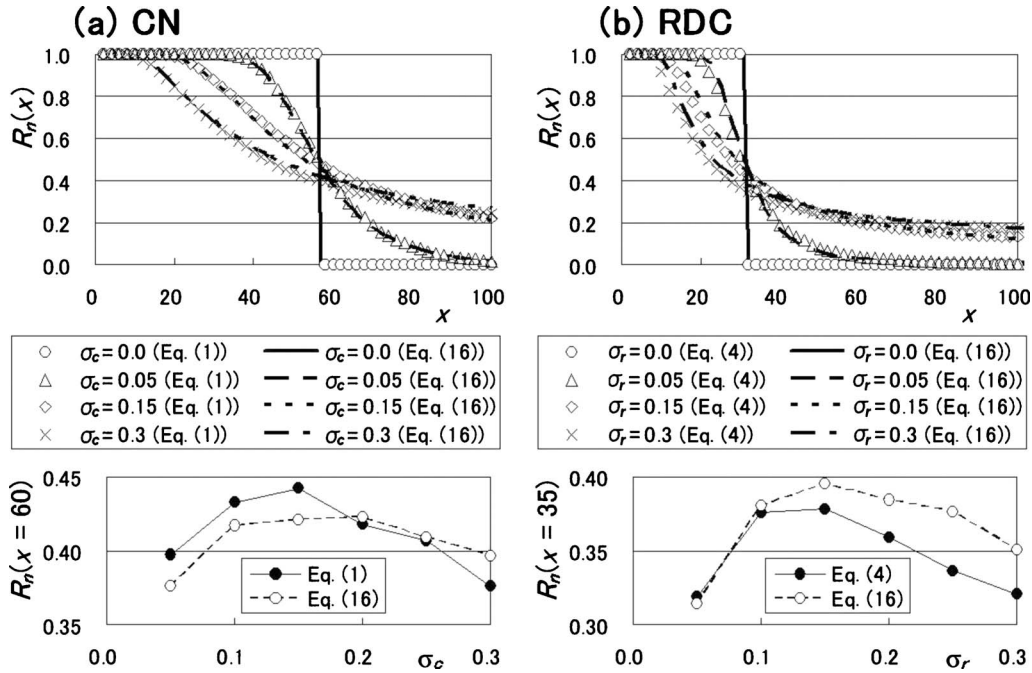
FIG. 9. Upper panels: Proportion $R_n(x)$ of survival pulses vs propagation length x in CN with $\tau_p=10.0$ and $\tau_s=4.0$ (a) and in RDC with $\tau_p=12.0$ and $\tau_s=5.0$ (b). Results of computer simulation with Eqs. (1) and (4) (symbols) and with Eq. (16) (lines). Lower panels: proportion $R_n(x)$ of survival pulses at $x=60$ in CN (a) and $x=35$ in RDC (b) vs noise strength.

though several kinds of measures including a spectrum-based SNR had been employed for showing optimal noise strength.

IV. CONCLUSION

Pulse propagation in two bistable systems with unidirectional flows in the presence of spatiotemporal additive white noise was studied. In a chain of unidirectionally coupled neurons pulses propagate in the direction of coupling, and in a reaction-diffusion-convection equation pulses propagate owing to convection. It is known that the propagation of pulses in both systems is described by qualitatively the same kinematical equation, which has an exponential deterministic term and a fluctuation term. Propagating pulses are unstable so that pulses disappear during propagation in the absence of noise, while the propagation length of pulses increases exponentially with pulse width.

In this paper the propagation length of a pulse in the presence of noise was formulated by the FPT for the stochastic kinematical equation. It was then shown that noise increases the mean propagation length of a pulse to infinity. The survival function of a pulse and the probability density function of the propagation length of a pulse have power-law tails as $x^{-1/2}$ and $x^{-3/2}$, respectively, when noise strength is sufficiently large, which are the same as those of the Wiener process. The optimal noise strength was also derived by imposing an upper bound of pulse width, and hence the resonancelike behavior exists intrinsically. Further, it was shown that the transmission rates of pulses in an asymmetric pulse train at fixed length increases in the presence of noise of intermediate strength. These resonancelike behaviors were observed in a range of not so large noise strength, in which

pulses still keep their forms and the existence and disappearance of pulses are clearly discriminated.

Noise-sustained pulse propagation with the same mechanism as shown in this paper can occur some other bistable systems with flows. For instance, it has been shown that unstable periodic solutions and transient oscillations similar to those in a ring neural network exist in a ring of unidirectionally coupled maps with cubic nonlinearity [20]. It has also been shown that noise enhances the transmission of subthreshold signals in a spatially discrete unidirectionally coupled bistable system [5] and noise improves performance of pulse transmission in a chain of forward-coupled bistable overdamped oscillators [8]. While these systems are expected to have kinematics of pulse propagation similar to CN and RDC, it has not been derived and remains in future work.

APPENDIX: EQUIVALENT STOCHASTIC PROCESSES

Kinematical Eq. (7) and the propagation length of a pulse are transformed to stochastic processes with multiplicative noise and FPT for them. We follow the Stratonovich rules according to [18] since they are the same as in ordinary calculus and the transformation of variables is valid. Values of the coefficients are set to $\alpha=\beta=1$ for simplicity, and the variable x corresponds to time in stochastic processes.

For a general stochastic process, $a(\tau)$ and $b(\tau)$ in Eq. (10) are given as

$$d\tau(x)/dx = f[\tau(x)] + g[\tau(x)]w(x)$$

$$a(\tau) = f(\tau) + \frac{1}{4}\frac{\partial g(\tau)^2}{\partial \tau}, \quad b(\tau) = g(\tau)^2, \qquad \text{(A1)}$$

(i) a stochastic process $y(x)$ with a quadratic term and multiplicative noise in a bounded domain $(0, 1)$

$$y(x) = \exp[-\tau(x)], \quad y(0) = \exp[-\tau(0)], \quad y(x_p) = 1$$

$$dy(x)/dx = y^2(x) + \sigma y(x)w(x) \quad (x > 0)$$

$$x_p[y(0); \sigma = 0] = 1/y(0) - 1 \quad [y(x_p) = 1]$$

$$a(y) = y^2 + \sigma^2 y/2, \quad b(y) = \sigma^2 y^2, \quad \pi(y) = \exp(-2y/\sigma^2)/y$$

$$m\{x_p[y(0)]\} = \frac{2}{\sigma^2} \int_{\exp[-\tau(0)]}^{1} d\eta \int_0^\eta d\xi \, \exp[2(\xi - \eta)/\sigma^2]/(\xi\eta).$$

$$(A2)$$

Initial values are exponentially small $(y(0) \ll 1)$ with initial pulse width $\tau(0)$. The quadratic deterministic term is then exponentially smaller than the fluctuation term, which makes the tendency of y toward unity unclear. Further, the fluctuation term is also exponentially small so that changes in the variable y are small for a long time. The double integral for the mean FPT diverges to infinity since the integrand is $O(1/\xi)$ for $\xi \to 0$.

(ii) A stochastic process $z(x)$ with a constant drift and multiplicative noise in a semi-infinite domain $(1, \infty)$,

$$z(x) = \exp[\tau(x)], \quad z(0) = \exp[\tau(0)], \quad z(x_p) = 1$$

$$dz(x)/dx = -1 + \sigma z(x)w(x) \quad (x > 0)$$

$$x_p[z(0); \sigma = 0] = z(0) - 1 \quad [z(x_p) = 1]$$

$$a(z) = -1 + \sigma^2 z/2, \quad b(y) = \sigma^2 z^2, \quad \pi(z) = \exp[-2/(\sigma^2 z)]/z$$

$$m\{x_p[z(0)]\} = \frac{2}{\sigma^2} \int_1^{\exp[\tau(0)]} d\eta \int_\eta^\infty d\xi$$
$$\times \exp[2(1/\xi - 1/\eta)/\sigma^2]/(\xi\eta). \quad (A3)$$

Initial values are exponentially large $(z \gg 1)$ with $\tau(0)$. Although there is a constant drift toward $z = 1$, the fluctuation term is exponentially large and overcomes the drift. Consequently the value of z remains large with large variations for a long time. The mean FPT diverges to infinity since the integrand is $O(1/\xi)$ for $\xi \to \infty$. Exponential nonlinearity and the resulting increases in the propagation length of a pulse in Eq. (7) are transferred to exponentially small Eq. (A2) or large Eq. (A3) initial values and multiplicative noise in both processes.

[1] L. Gammaitoni *et al.*, Rev. Mod. Phys. **70**, 223 (1998); B. Lindner *et al.*, Phys. Rep. **392**, 321 (2004); F. Sagués, J. M. Sancho, and J. García-Ojalvo, Rev. Mod. Phys. **79**, 829 (2007).

[2] M. Loecher, *Noise Sustained Patterns: Fluctuations and Non-linearities* (World Scientific, Singapore, 2002).

[3] P. Jung and G. Mayer-Kress, Chaos **5**, 458 (1995).

[4] M. Löcher, D. Cigna, and E. R. Hunt, Phys. Rev. Lett. **80**, 5212 (1998).

[5] Y. Zhang, G. Hu, and L. Gammaitoni, Phys. Rev. E **58**, 2952 (1998).

[6] J. F. Lindner *et al.*, Phys. Rev. Lett. **81**, 5048 (1998).

[7] F. C. Blondeau and J. R. Varela, Int. J. Bifurcation Chaos Appl. Sci. Eng. **10**, 1951 (2000).

[8] S. A. Ibáñez *et al.*, Physica D **238**, 2138 (2009).

[9] J. García-Ojalvo *et al.*, Europhys. Lett. **50**, 427 (2000).

[10] S. Amari, *Mathematics of Neural Networks (in Japanese)* (Sangyo-Tosho, Tokyo, 1978); M. H. Hirsh, Neural Networks **2**, 331 (1989); A. F. Atiya and P. Baldi, Int. J. Neural Syst. **1**, 103 (1989); P. Baldi and A. F. Atiya, IEEE Trans. Neural Netw. **5**, 612 (1994); K. Pakdaman *et al.*, Phys. Rev. E **55**, 3234 (1997); T. Gedeon, *Cyclic Feedback Systems, Memoirs of the American Mathematical Society* (AMS, Providence, 1998).

[11] Y. Horikawa and H. Kitajima, Physica D **238**, 216 (2009).

[12] Y. Horikawa and H. Kitajima, Phys. Rev. E **80**, 021934 (2009).

[13] K. Kawasaki and T. Ohta, Physica A **116**, 573 (1982); J. Carr and R. L. Pego, Commun. Pure Appl. Math. **42**, 523 (1989) see especially p. 545; S. Ei and T. Ohta, Phys. Rev. E **50**, 4672 (1994).

[14] Y. Horikawa, Phys. Rev. E **78**, 066108 (2008).

[15] Y. Horikawa, Neurocomputing (to be published).

[16] A. S. Mikhailov, L. Schimansky-Geier, and W. Ebeling, Phys. Lett. A **96**, 453 (1983).

[17] W. Feller, *An Introduction to Probability Theory and Its Applications 1*, 3rd ed. (John Wiley & Sons, New York, 1968).

[18] N. S. Goel and N. Richter-Dyn, *Stochastic Models in Biology* (Academic Press, New York, 1974).

[19] H. C. Tuckwell, *Stochastic Processes in the Neurosciences* (SIAM, Philadelphia, 1989).

[20] H. Kitajima and Y. Horikawa, *Proceedings of the 2007 International Symposium on Nonlinear Theory and its Applications*, edited by L. Trajkovic and K. Okumura (IEICE, Tokyo, 2007).